

Statistics of magnetic field measurements in OBA stars and the evolution of their magnetic fields

A. S. Medvedev^{1,*}, A. F. Kholtygin^{2,**}, S. Hubrig³, M. Schöller⁴, S. Fabrika^{1,5}, G. G. Valyavin¹, G. A. Chountonov¹, Yu. V. Milanova², O. A. Tsiopa⁶, and V. A. Yakovleva²

¹ Special Astrophysical Observatory, Nizhnii Arkhyz, Russia

² Saint-Petersburg University, Russia

³ Leibniz-Institut für Astrophysik Potsdam (AIP), Potsdam, Germany

⁴ European Southern Observatory, Garching, Germany

⁵ Kazan Federal University, Kazan, Russia

⁶ Main (Pulkovo) Observatory, Saint-Petersburg, Russia

Received 2017, accepted 2017

Published online later

Key words stars: early-type - stars: magnetic fields - stars: statistics

We review the measurements of magnetic fields of OBA stars. Based on these data we confirm that magnetic fields are distributed according to a lognormal law with a mean $\log B = -0.5$ (B in kG) with a standard deviation $\sigma = 0.5$. The shape of the magnetic field distribution is similar to that for neutron stars. This finding is in favor of the hypothesis that the magnetic field of a neutron star is determined mainly by the magnetic field of its predecessor, the massive OB star. Further, we model the evolution of an ensemble of magnetic massive stars in the Galaxy. We use our own population synthesis code to obtain the distribution of stellar radii, ages, masses, temperatures, effective magnetic fields, and magnetic fluxes from the pre-main sequence via zero age main sequence (ZAMS) up to the terminal age main sequence stages. A comparison of the obtained in our model magnetic field distribution (MFD) with that obtained from the recent measurements of the stellar magnetic field allows us to conclude that the evolution of magnetic fields of massive stars is slow if not absent. The shape of the real MFD shows no indications of the *magnetic desert* proposed previously. Based on this finding we argue that the observed fraction of magnetic stars is determined by physical conditions at the PMS stage of stellar evolution.

Copyright line will be provided by the publisher

1 Introduction

Knowledge of the properties of the magnetic fields in massive stars is very important for our understanding the mechanisms of their formation and evolution as well as their impact on the stellar parameters and evolution. Accurate studies of the age, environment, and kinematic characteristics of magnetic stars are promising to give us new insight into the origin of the magnetic fields (e.g. Hubrig et al. 2011, 2013; González et al. 2017).

For a number of early B-type stars the magnetic fields were detected several tens of years ago (e.g. Babcock 1947). The first magnetic field detection in an O-type star was made in 2002 by Donati et al. (2002), even though the existence of magnetic O-type stars had been suspected for a long time.

The recent systematic surveys MiMeS (The Magnetism in Massive Stars) and BOB (The B fields in OB stars) aiming at the detection and studying of the magnetic fields in massive stars (Wade et al. 2016; Morel et al. 2014) strongly

enhanced the number of known magnetic OBA stars in comparison with ~ 500 OBA stars with confirmed magnetic field which were known before 2009 (e.g. Bychkov et al. 2009). Because of the increase in the number of new detections it was also found that incidence of massive magnetic stars is about of 7% only (Wade et al. 2014).

The detection rate obtained by the BOB collaboration is of $6 \pm 4\%$ (Schöller et al. 2017) which is consistent with that given by the MiMeS group.

Measuring the magnetic fields of hundreds of OBA stars opens the possibility to study the magnetic field distribution for different types of stars (e.g., Kholtygin et al. 2010a). The understanding of the nature of the magnetic field of massive stars can be based on our knowledge of their MFD. Checking the real MFD showed that some previous ideas about the magnetic field evolution can be incorrect.

For example, the MFD predicted by Ferrario & Wickramasinghe (2006) for massive stars on the main sequence in the mass range from 8 to $45 M_{\odot}$ based on the hypothesis that the net magnetic flux for a massive star and its descendant, the neutron star, is the same (see their Fig. 4) does not agree with the real distribution of the magnetic field (e.g. Kholtygin et al. 2010a).

* A. S. Medvedev: e-mail: a.s.medvedev@gmail.com

** A. F. Kholtygin: e-mail: afkholtygin@gmail.com

The disagreement between the predicted MFD and the one based on the real measurements is connected with the dissipation of the stellar magnetic flux during the evolution from massive stars to neutron stars (see Fig. 1 in the paper by Igoshev & Khoitygin 2011 and subsection 3.5 in the present paper). It is shown that the magnetic fluxes of neutron stars are about of three orders of magnitude lower than for their progenitors, the massive OB stars.

It means that the studying how the magnetic fields and the magnetic fluxes change during the massive star evolution plays a decisive role in the understanding the nature of the magnetic field of this group of stars. In the present paper we consider the evolution of the magnetic fields and fluxes of OBA stars at the main sequence stage.

Our paper is organized in the following way: The accepted model of the evolution of magnetic OBA stars is described in Sect. 2. In Sect. 3 we review the empirical magnetic field distributions of OBA stars. In Sect. 4 we discuss the *magnetic desert* problem and give some constrains on the rate of dissipation of stellar magnetic fields. Finally we summarize our results and give some conclusions in Sect. 5.

2 The Model

2.1 Population synthesis

Information about the intrinsic distribution of stellar magnetic fields can only be obtained from an analysis of observations of certain sample of stars. Even the stars of the same spectral class and even subclass have significant diversity in masses, ages and other characteristics. These characteristics influence the magnitude of a large-scale magnetic field due, for example, the geometrical effects and the dissipation processes. Therefore, to simulate the magnetic field distribution for the model ensemble of stars, these variations in the stellar parameters have to be taken into account. Here we outline the main features of our population synthesis model realizing this aim.

The first step of our modeling is a creation of the initial ensemble of stars. We suppose that a total number of stars in the ensemble is N_{tot} and the stellar masses $M \in [M_{\text{min}}, M_{\text{max}}]$. The mass distribution at the ZAMS is described by a power law with an exponent of -2.3 . This corresponds to the high-mass region of the stellar initial mass function (Kroupa 2002). The appearance time t_* of an each star at ZAMS is generated randomly using the uniform distribution in the range $t_* \in [0, T]$, where T is the total simulation time. We use the constant stellar birthrate λ .

This means that approximately one star appears in the time interval $\Delta T = 1/\lambda$. The simulation time T has to be at least three times longer than the main sequence lifetime τ_{MS} of a least massive star in the ensemble to be sure that the model star ensemble is stationary.

Next steps include the computation of stellar parameters and selection of the stars remaining on the main sequence at

the moment of time T . Evolution of the stars in the ensemble is simulated using the rapid single-star evolution code SSE developed by Hurley et al. (2000). This code is based on analytical approximations of evolutionary tracks computed by Pols et al. (1998). It can be used for simulations of all stages of stellar evolution from the ZAMS to final remnants and it is valid for masses in the range $0.1\text{--}100 M_{\odot}$.

Our population synthesis code is created on the base of the Astrophysical Multipurpose Software Environment (AMUSE) developed by Pelupessy et al. (2013). The platform AMUSE uses *python* as an interface between different existing astrophysical codes (stellar dynamics, stellar evolution, hydrodynamics, etc.) and provides a framework in which these codes can be coupled¹.

2.2 Evolution of stellar magnetic fields

2.2.1 Basic definitions

In our model the magnetic field of a star is defined via the net magnetic flux Φ at the stellar surface:

$$\Phi = \int_S |B_r| dS. \quad (1)$$

Here B_r is the radial projection of the B -field and dS is a surface element. This parametrization is very useful for describing the magnetic properties of stellar populations because the assumption about of the conservation of magnetic flux in the absence of dynamo or dissipation mechanisms is very good (e.g. Braithwaite & Nordlund 2006).

In the case of a dipole field the relation between the net magnetic flux Φ_d and the polar field B_d can be easily derived:

$$\Phi_d = 4/3\pi B_d R^2, \quad (2)$$

where R is a radius of a star. However, current techniques used to measure stellar magnetic fields can give us only the longitudinal component B_l of the field. Although B_l is directly connected to the polar field B_d , it also depends on the rotation phase ϕ , angle between the magnetic dipole and rotation axes β , and the inclination of the rotation axis to the line of sight i (e.g. Preston 1967). The later two parameters are completely random and have a wide range of possible values. Even the phase-averaged field $\langle B_l \rangle_{\phi}$ is very sensitive to their variations.

Because of these reasons, we use the root-mean-square (*rms*) field \mathcal{B} instead of B_d as the main characteristic of stellar magnetic fields. If N is the total number of the field measurements B_l^k ($k = 1 \dots N$), then the *rms*-field is given by the formula (e.g. Bohlender et al. 1993):

$$\mathcal{B} = \sqrt{\frac{1}{N} \sum_{k=1}^n (B_l^k)^2}. \quad (3)$$

¹ see <http://www.amusecode.org> for details

The phase-averaged ratio B/B_d and its asymptotical behavior at $N \rightarrow \infty$ were investigated by Kholtygin et al. (2010a). They demonstrated that in the case of a dipole configuration the *rms*-field \mathcal{B} weakly depends on random values of the rotational phase ϕ , inclination i and the angle β . This conclusion also is valid for quadrupole and more complex field configurations. Following this paper we adopt that

$$\mathcal{B} \approx 0.2B_d. \quad (4)$$

Then we can find the net magnetic flux using next relation:

$$\Phi = 4\pi R^2 \mathcal{B}. \quad (5)$$

It gives a good estimation of the net magnetic flux for any field configurations (Kholtygin et al. 2010a).

2.2.2 Magnetic field function at ZAMS

In order to simulate the evolution of stellar magnetic fields with the stellar age t it is necessary first to define the initial magnetic field function for the stars at the ZAMS ($t = 0$). We assume the lognormal distribution of the net magnetic fluxes:

$$f(\Phi | t = 0) = \frac{A}{\Phi\sigma} \exp \left\{ -\frac{1}{2} \left(\frac{\log \Phi - \langle \log \Phi \rangle}{\sigma} \right)^2 \right\}, \quad (6)$$

where Φ is the net magnetic flux, $\langle \log \Phi \rangle$ is the mean value of the $\log \Phi$, σ is the width (in dex) of the distribution and

$$A = \frac{1}{\sqrt{2\pi} \ln 10}. \quad (7)$$

We chose the lognormal distribution of the magnetic fluxes mainly due to similarity between lognormal and empirical distributions derived from real samples of magnetic stars (this similarity is discussed in Section 3). A lognormal magnetic flux distribution (magnetic flux function) may be obtained from the simple assumption that during the pre-main sequence evolution the magnetic field of a star is experiencing a finite number of cycles of amplification/damping by some random factor. Under rather wide conditions the resulting magnetic field function will coincide to a lognormal distribution even for a small number of the cycles (see Kholtygin et al. 2016 for details).

2.2.3 Dissipation of magnetic fields

Observational evidences imply that the magnetic fields of Ap stars decay. The rate of dissipation depends strongly on stellar mass (e.g. Landstreet et al. 2008). According to Kholtygin et al. (2010b) the dissipation of magnetic fields can be represented as the exponential function $\propto e^{-\alpha_d \tau}$, where τ is the age of a star expressed in terms of the main sequence lifetime of the star, and $\alpha_d \sim 2.0$ is the dissipation factor. We also assume exponential decay of stellar

magnetic fields on the time-scale t_d which is set to be proportional to the lifetime of a star on the main sequence t_{MS} . Introducing the dissipation parameter as

$$\tau_d = \frac{t_d}{t_{MS}}, \quad (8)$$

we obtain the following expression for the temporal evolution of the net magnetic flux:

$$\Phi(t) = \Phi(0) \exp \left\{ -\frac{1}{\tau_d} \left(\frac{t}{t_{MS}} \right) \right\}. \quad (9)$$

The time dependence of the *rms*-field $B(t)$ can be derived from this relation and by using the formula (5).

2.3 Random sampling and parameter estimation

2.3.1 Generation of empirical distributions

To derive an empirical magnetic fields distribution from a sample consisting of N_{smp1} stars, the first step is to split the entire range of magnetic fields into a set of N_{bins} equally-sized intervals (bins) and then count how many stars fall into each bin. Obviously, large samples are more preferable for obtaining empirical distributions which would accurately resemble the intrinsic magnetic field function. Unfortunately, the current number of known magnetic stars is still very limited, therefore it is important to understand i) how the *intrinsic* model magnetic field function would manifest itself as empirical distribution and ii) how the number of stars in a sample affects the magnitude of possible variations in distribution function due to statistical effects. For these purposes we developed the random sampling method which allows to produce empirical distributions from the model.

The random sampling is used to generate a large set of equally-sized samples from the ensemble of magnetic stars created by the population synthesis module (see Section 2.1). Then distributions of magnetic fields in each of the samples are passing through the special procedure to obtain average distribution as well as confidence boundaries for the uncertainties in a counts number for each of the defined bins.

If $n_k(i)$ is the number of stars in i -th bin of k -th sample then the averaged number of stars in the bin is

$$\langle n(i) \rangle = \frac{1}{N_{\text{smp1}}} \sum_{k=1}^{N_{\text{smp1}}} n_k(i), \quad (10)$$

where N_{smp1} is the number of generated samples. The confidence boundaries for a desired level of significance are calculated using the Poisson statistics.

2.3.2 Parameter estimation

Since real samples of massive magnetic stars are small, the standard χ^2 statistics is no longer valid for the parameter es-

Table 1 List of the main model parameters.

#	Quantity	Units	Description
1.	M_{\min}, M_{\max}	M_{\odot}	Mass interval limits
2.	N_{smp1}		Number of stars in a sample
3.	$\langle \log \Phi \rangle$	G-cm ²	Mean magnetic flux at the ZAMS
4.	σ	dex	Width of the initial distribution
5.	τ_d	t_{MS}^a	Time-scale of the magnetic field

^a Lifetime of a star on the main sequence.

timization. For this reason, instead of χ^2 we use the C statistics in form

$$C_q = 2 \sum_{i=1}^{N_{\text{bins}}} [e_i - n_i + n_i(\ln n_i - \ln e_i)], \quad (11)$$

where n_i is a number of stars in each of the bins of the empirical distribution, e_i is the expected number of stars given by the model, and N_{bins} is a number of bins. The C statistics were introduced by Cash (1979) as replacement of χ^2 that would be valid even for a very small samples. It is commonly used in X-ray and gamma-ray astronomy in cases when the number of photons received by a detector is low.

The following method is used for generating confidence intervals for the model parameters. First, we find the minimum value $(C_q)_{\min}$ when the model is fitted to the data and q parameters are varied. Then, assuming the level of significance α , we determine the locus of points in parameter space for which

$$C - (C_q)_{\min} > \Delta C(\alpha). \quad (12)$$

According to Cash (1979) the ΔC statistics can be represented as

$$\Delta C(\alpha) = \chi_q^2(\alpha) + O\left(\frac{1}{\sqrt{N_{\text{smp1}}}}\right), \quad (13)$$

where N_{smp1} is the total number of stars in a samples. For $N_{\text{smp1}} \gg 1$ the ΔC statistics follows the χ^2 distribution for q degrees of freedom. However, we generate the distribution of ΔC from our model using the Monte Carlo simulations, because the term $O(N_{\text{smp1}}^{-1/2})$ cannot be neglected when $N_{\text{smp1}} \lesssim 10$.

The C statistics may also be easily modified for the purpose of simultaneous fitting of different datasets.

2.4 Parameters of the model

A short summary describing the main parameters of the model is presented in Table 1. Note that two of the parameters such as the mass interval $[M_{\min}, M_{\max}]$ and the sample size N_{smp1} , may be determined directly from characteristics of empirical data. For example, an empirical magnetic

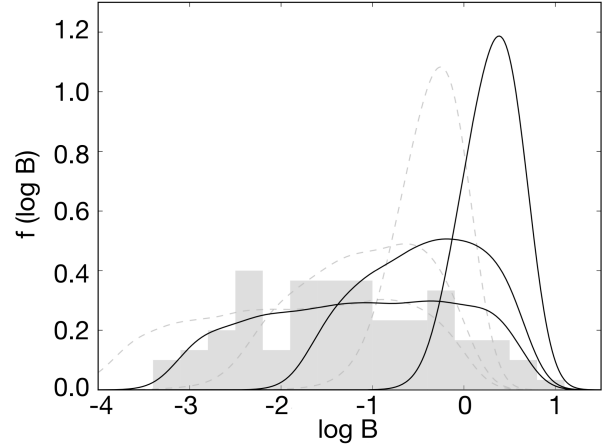


Fig. 1 Magnetic field function of early-type stars calculated using our model. Black lines correspond to different values of the dissipation parameter $\tau_d = 0.15$ (left curve), 0.3 (central curve), and ∞ (right curve) in Eq.8. All distributions are obtained from the stellar ensemble containing stars with masses in the range 2–10 M_{\odot} and following parameters of the net magnetic flux distribution at the ZAMS: $\langle \log \Phi \rangle = 27.5$, $\sigma = 0.2$ (see Eq.6 for detail). Dashed lines show the distributions calculated using the same parameters but for the mass range 10–60 M_{\odot} . The gray histogram represents a single realization of the empirical distribution ($\tau_d = 0.15$) for the small ensemble with $N_{\text{smp1}} = 100$ for the initial masses in the 2–10 M_{\odot} range. The magnetic field strength B is given in kG.

fields distribution derived from a sample of eleven O-type stars suggests that $M \in [16, 60] M_{\odot}$ and $N_{\text{smp1}} = 11$. The remaining three parameters however have to be estimated from fitting of the empirical data.

Some examples of magnetic field functions produced by the model are presented in Fig. 1. Such parameters as $\langle \log \Phi \rangle$ and σ define the position and overall width of the magnetic fields function. The mass interval influences some minor asymmetry in the shape of the magnetic field function due to changes of stellar radii during evolution on the main sequence. The dissipation parameter τ_d has the most profound impact on a magnetic field function. In the case of no dissipation of magnetic fields, or if $\tau_d \gg 1$, the magnetic field function would be a bell-shaped curve, with some minor asymmetry. However, if the magnetic field decay is fast ($\tau_d \ll 1$), the model would produce a highly asymmetrical magnetic field function. Finally, the sample size parameter N_{smp1} defines possible manifestations of a magnetic field function as an empirical distribution derived from a finite number of magnetic fields measurements.

3 Analysis of the empirical magnetic field distributions for OBA stars

3.1 Magnetic field measurements

In order to compare our model with observations, we first divided all known magnetic stars into three groups: BA stars (this groups contains mainly Ap/Bp stars), O and early B type stars combined together (OB stars), and O type stars only. These groups correspond to the mass ranges 1.5–16, 3–16 and 16–60 M_{\odot} .

Magnetic field measurements for BA stars were taken from the catalogue by Bychkov et al. (2009) which contains hundreds of magnetic stars. However only 288 stars with most reliable measurements were selected, based on statistical criteria described by Kholtygin et al. (2011a). The data for O- and early B-type stars were compiled from multiple sources (Petit et al. 2013; Fossati et al. 2014, 2015a, 2015b; Alecian et al. 2014; Castro 2015) with the total amount of 73 stars, including 11 O-type stars.

If only dipolar magnetic field strengths B_d were given in the used sources, we converted them to *rms* magnetic field \mathcal{B} via relation (4). The empirical magnetic field distribution $f(\mathcal{B})$ for the sample of stars with measured magnetic fields was introduced by Fabrika & Valyavin (1999) and Monin et al. (2002). It equals to

$$f(\mathcal{B}) \approx \frac{N(\mathcal{B}, \mathcal{B} + \Delta\mathcal{B})}{N_{\text{tot}}\Delta\mathcal{B}}, \quad (14)$$

where $N(\mathcal{B}, \mathcal{B} + \Delta\mathcal{B})$ is the number of stars with the *rms* magnetic fields \mathcal{B} in the interval $(\mathcal{B}, \mathcal{B} + \Delta\mathcal{B})$ and N_{tot} is the total number of stars with measured *rms* magnetic field.

3.2 BA stars

The empirical distribution of magnetic fields derived from our sample of BA stars is presented in Fig. 2. It is bell-shaped with a maximum located at $\mathcal{B} \approx 300$ G, and may be easily approximated by lognormal distribution. In Section 2.4 we found that the shape of the model distribution was highly dependent on the value of the dissipation parameter (see also Fig. 1). Therefore, one may expect that τ_d has to be large to produce the symmetrical magnetic field functions which would be consistent with the empirical data in Fig. 2. At the same time the maximal symmetry would be achieved only if the dissipation parameter was infinite. Thus we decided to consider two models: i) the model \mathcal{M}_0 in which we assume no dissipation of stellar magnetic fields, i.e. $\tau_d \rightarrow \infty$; ii) the model \mathcal{M}_1 with a dissipation and a finite value of τ_d .

We find that the model \mathcal{M}_0 is in a good agreement with the empirical magnetic field distribution for BA stars (see Fig. 3, top panel). The parameters of the best-fit and the corresponding confidence intervals as well as the value of the C statistics are presented in Table 2.

Applying the model \mathcal{M}_1 for the analysis of the empirical data we discovered that from a statistical point of view

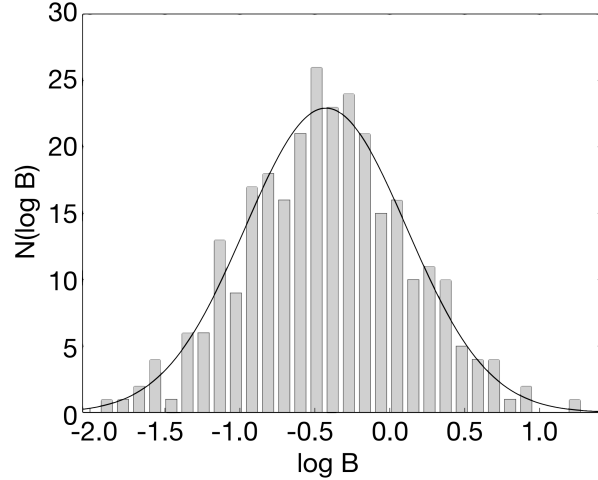


Fig. 2 Magnetic field distribution for BA stars (gray histogram) $N = N(\mathcal{B}, \mathcal{B} + \Delta\mathcal{B})$. The distribution is derived using the measured magnetic field data by Bychkov et al. (2009). Black line represents the lognormal distribution with $\langle \log B \rangle \approx -0.5$ (B in kG) and $\sigma \approx 0.5$ dex.

Table 2 Parameters of the best fitting models for magnetic field distribution functions of BA and OB stars.

	Model	$\langle \log \Phi \rangle$ G cm ²	σ_0	τ_d	C/n_{bins}	p_{null}
BA	\mathcal{M}_0	26.42 ^{+0.04} _{-0.04}	0.5 ^{+0.04} _{-0.05}	∞	14.84/30	0.96
	\mathcal{M}_1	26.83 ^{+0.07} _{-0.06}	0.33 ^{+0.04} _{-0.07}	0.5	22.2/30	0.37
OB	\mathcal{M}_0	26.51 ^{+0.11} _{-0.15}	0.53 ^{+0.07} _{-0.11}	∞	13.78/18	0.72
	\mathcal{M}_1	26.9 ^{+0.13} _{-0.17}	0.47 ^{+0.08} _{-0.17}	0.5	16.5/18	0.3
O	\mathcal{M}_0	26.95 ^{+0.35} _{-0.45}	0.52 ^{+0.18} _{-0.49}	∞	2.67/5	0.35
	\mathcal{M}_1	27.29 ^{+0.47} _{-0.59}	0.51 ^{+0.04} _{-0.1}	0.5	3.58/5	0.3
Simultaneous fitting						
OBA	\mathcal{M}_0	26.45 ^{+0.05} _{-0.05}	0.5 ^{+0.04} _{-0.05}	∞	48.3/53	0.73
	\mathcal{M}_1	26.87 ^{+0.05} _{-0.07}	0.35 ^{+0.04} _{-0.09}	0.5	48.3/53	0.43

the results were equally good for any value of the dissipation parameter taken from the range $\tau_d \gtrsim 0.5$. Below this threshold the quality of fitting is rapidly decreasing beyond acceptable limits. Thus we conclude that $\tau_d = 0.5$ corresponds to the highest rate of magnetic field decay allowed by the agreement with the empirical distribution of BA stars. We assume this value for the further analysis using \mathcal{M}_1 model.

The model \mathcal{M}_1 which provide the best fit of the empirical distribution of BA stars magnetic fields is given in Fig. 3 (bottom panel). Like the model \mathcal{M}_0 it also gives a good agreement with the data but it also possess the higher

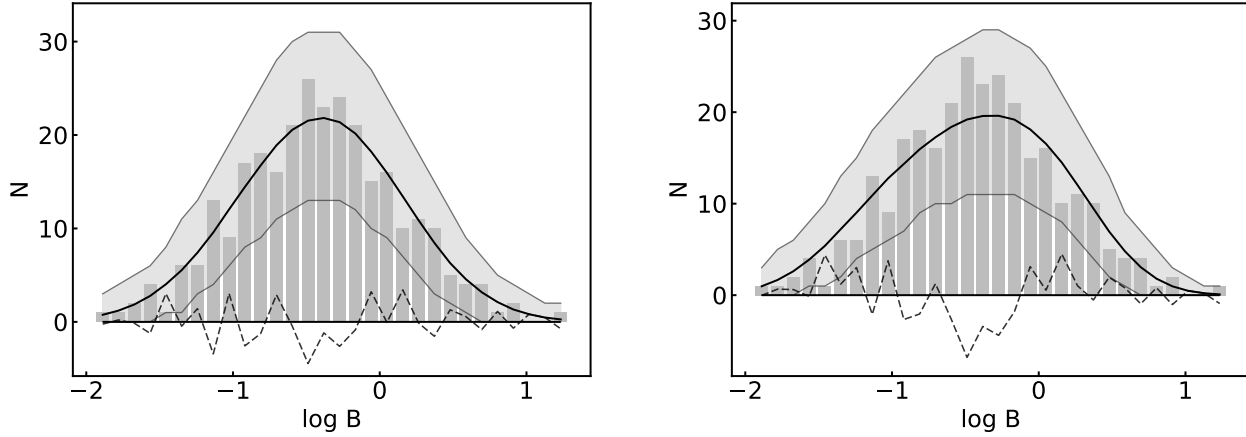


Fig. 3 *Right panel.* Model \mathcal{M}_0 (thick black line) in comparison with the empirical magnetic field distribution for BA stars (grey histogram). The dashed line represents the residuals which are the difference between the model and the observed distribution. The model distribution is calculated for the parameters providing the best fit $\langle \log \Phi \rangle = 26.42$, $\sigma = 0.5$. The dissipation parameter $\tau_d = \infty$. The gray filled area corresponds to the 95 % confidence interval for the possible variations of the sampled magnetic field distribution with upper and lower limits represented by the thin grey lines. *Left panel.* The same but for the model \mathcal{M}_1 . The parameters of the best fit are $\langle \log \Phi \rangle = 26.83$ and $\sigma = 0.33$. The dissipation parameter is fixed at $\tau_d = 0.5$.

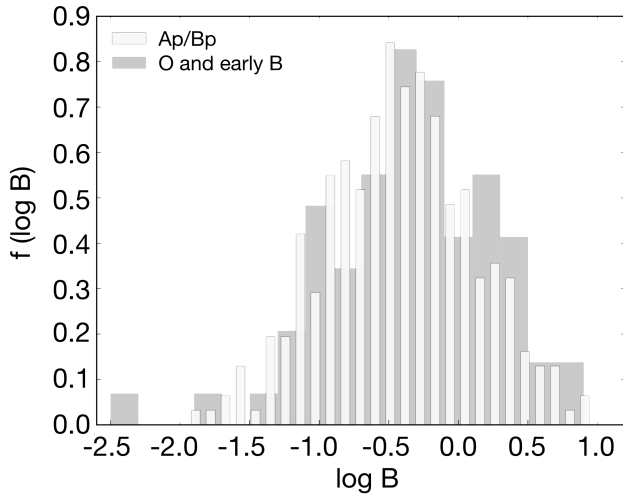


Fig. 4 Normalized magnetic field distributions for BA (white histogram) and OB stars (gray histogram). Magnetic field strengths for BA stars were taken from Bychkov et al. (2009). For OB stars data from multiple sources were used (Section 3.1). Both distributions have the same bell-shaped appearance, location of maximum and spread.

and less scattered values of the net magnetic flux $\langle \log \Phi \rangle$ for stars at the ZAMS as it seen in Table 2.

3.3 OB stars

The empirical magnetic field distribution of O- and early B-type stars is very similar in appearance to that of BA stars. The resemblance becomes obvious from Fig. 4 in which these distributions are presented together. This is why first

we used the previously obtained for BA stars best-fitting parameters to calculate the model distribution of OB stars. Thus, we confirmed our hypothesis that both empirical distributions are likely drawn from the same intrinsic magnetic field function (the corresponding p -values for two of the models are $p_{\text{null}}(\mathcal{M}_0) = 0.4$ and $p_{\text{null}}(\mathcal{M}_1) = 0.31$).

Both the model \mathcal{M}_0 and model \mathcal{M}_1 are in a good agreement with the empirical magnetic field distribution for OB stars (see Fig. 5). The parameters of the best-fit and the corresponding confidence intervals as well as the value of the C statistics are presented in Table 2. We compared the proper best-fitting parameters for OB stars with those obtained for BA stars (Table 2). We also find that both models give a good agreement with the data (Fig. 4). Therefore we can conclude that the results of our analysis strongly imply a close similarity between the magnetic field distribution for BA and OB stars.

3.4 O stars and OBA stars

Up to date the number of known O-type magnetic stars is still very small. Consequently, it is virtually impossible to make reliable estimates of the parameters describing the corresponding magnetic field function from the available data because of large uncertainties of counting statistics. Nevertheless, we applied the same procedure as before and found the best-fitting parameters for the models \mathcal{M}_0 and \mathcal{M}_1 . A comparison of the model and the empirical magnetic field distributions for O stars and for the models \mathcal{M}_0 and \mathcal{M}_1 is given in Fig. 6.

We obtained significantly higher values for $\langle \log \Phi \rangle$ in comparison to the other groups of stars, although the estimated 95% confidence intervals for the model parameters

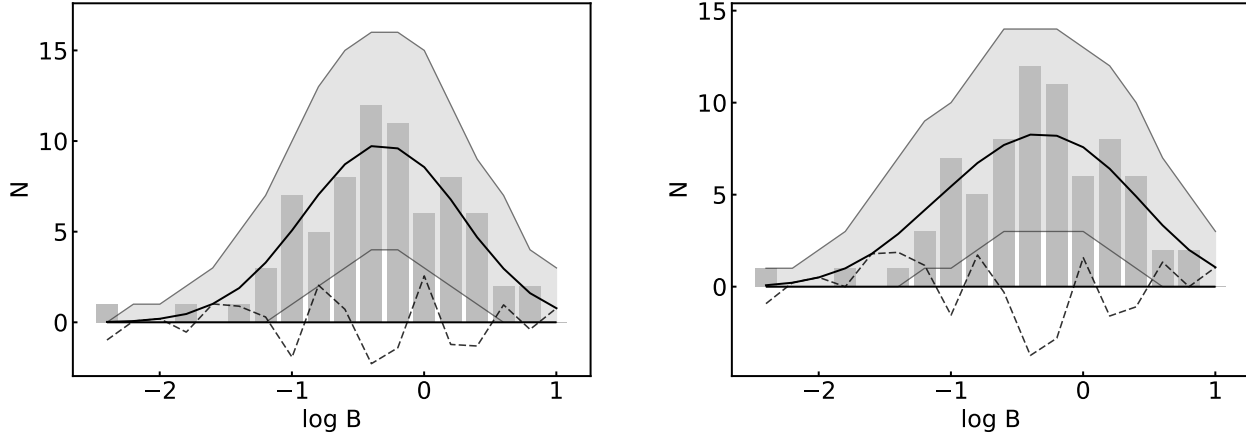


Fig. 5 Same as in Fig. 3, but for O- and early B-type stars.

are turned to be also much wider (Table 2). The null hypothesis that the empirical magnetic field distribution of O-type stars is drawn from the same magnetic field function as the distributions of BA and OB stars gives the p -value of 0.1, which is quite low but still higher than the commonly accepted rejection value of 0.05.

In order to test further the hypothesis that all of the empirical distributions could be drawn from a single magnetic field function, we applied the technique of simultaneous fitting, which was described above in Section 2.3.2 to all sample of OBA stars including the individual subsamples of BA, OB and O stars considered above. The results of the fitting are listed in the last 2 rows of Table 2. This result supports our hypothesis on the similarity of all of the considered empirical distributions. It means that the magnetic field distribution for OBA stars obeys a common distribution law.

3.5 Magnetic Flux distribution

In this subsection we outline the evolution of magnetic field of the massive stars after the main sequence. In Fig. 7 we present the magnetic fluxes distributions for OB stars, Wolf-Rayet (WR) stars and different types of the neutron stars (NSs). For OB stars we took the value of *rms* magnetic fields from the catalogue by Bychkov et al. (2009). The radii of stars were taken either from the original papers for considered stars or from the CADARS Catalogue (Pasinetti Fracassini et al. 2001).

All known galactic NSs were divided into three groups: normal pulsars, milliseconds pulsars, and magnetars. The data for neutron stars are taken from the ATNF Pulsar Catalogue (Manchester et al. 2005) and SGR/AXP Online Catalog. We put for all NSs the standard radius $R_* = 10$ km. The distribution of the magnetic fluxes both for these groups of neutron stars and for OB stars are the same what was presented by Igoshev & Kholtygin (2011) in their Fig. 1.

We add to their data the distribution of the upper limits of the magnetic fluxes for WR stars. The upper limits

of magnetic fields for 11 WR stars was taken from the paper Chevrotière et al. (2014). The upper limit of the magnetic field for the star WR 136 is given by Kholtygin et al. (Kholtygin et al. 2011b) and for WR 6 by Hubrig et al. (2016). For all WR stars we use the standard radius $R_* = 5R_\odot$.

We can see in Fig. 7 that although the width of distributions for NSs are close to that for OB stars, the mean fluxes are very different. The youngest group of NS (magnetars) has the largest fluxes, while the magnetic fluxes of the oldest NS (millisecond pulsars) are on the average smaller by 7 orders-of-magnitude. The mean fluxes of all remaining NSs (Normal pulsars) have intermediate values. We see that the mean fluxes of all types of NSs, excluding magnetars, are much lower than the mean fluxes of their progenitors, viz. the massive OB stars.

On the other hand, the upper limits of the magnetic fluxes for WR stars are close to those for normal pulsars. It means that the main dissipation of the magnetic flux during the evolution from the main sequence massive OB stars occurs between the ZAMS and the WR stage. At the same time, this can mean that the changes of the magnetic fluxes during of the supernova explosion are relatively small in agreement with the hypothesis by Ferrario & Wickramasinghe (2006).

4 Discussion

4.1 The “magnetic desert” problem

Lignières et al. 2014 proposed a scenario whereby the magnetic dichotomy between BA and Vega-like magnetism originates from the bifurcation between stable and unstable large scale magnetic configurations in differentially rotating stars. This means that the number of BA (and possibly O) stars with the *rms*-magnetic fields in interval between ~ 1 G and ~ 300 G is small if not negligible.

At the same time the empirical magnetic field functions obtained by us for OB and BA stars reveal that the same reg-

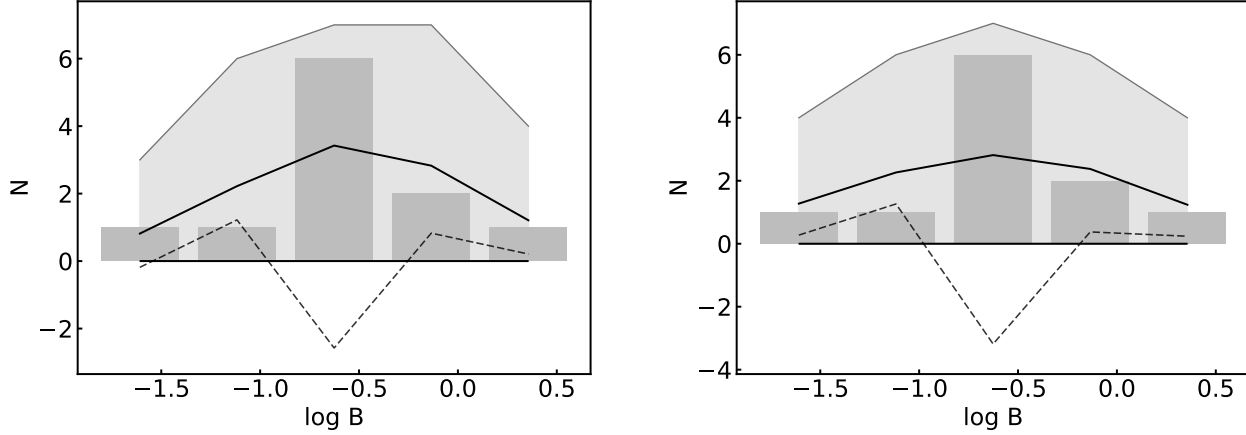


Fig. 6 Same as in Fig. 3, but for O-type stars.

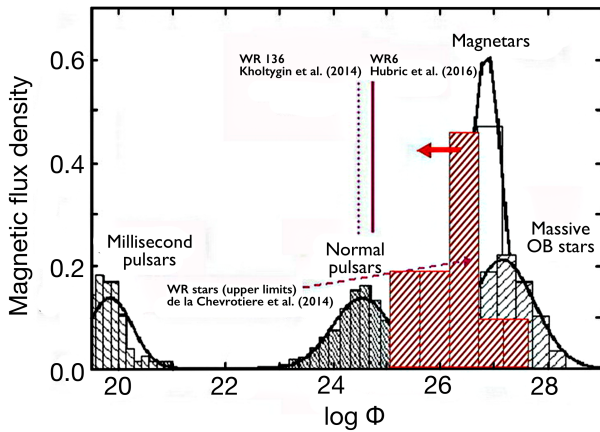


Fig. 7 The distribution of magnetic fluxes for massive OB stars, magnetars, and normal and millisecond (thick black lines and dashed histograms). Red dashed histogram shows the distribution of the upper limits of the magnetic fluxes for WR stars (using the red arrow we note that the real distribution would be shifted towards smaller values of magnetic flux). The upper limits of the magnetic fluxes for WR 6 and WR 136 are shown by solid and dotted red lines, respectively.

ular shape can be fitted by a lognormal distribution. There are no visible peculiarities that might indicate the existence of a threshold magnetic field reported for BA and early B-type stars by Aurière et al. (2007) and by Kholtygin et al. (2010a). The cumulative distributions produced by truncated magnetic field functions are too steep in comparison to the empirical ones (see Fig. 8).

The same issue also has been discussed by Fossati et al. (2015a), who reported the detection of weak magnetic fields (below 100 G) in two early B-type stars: β CMa (HD 44743) and ϵ CMa (HD 52089). The estimated upper limit for a dipolar field strength of the latter star is $B_d \gtrsim 13$ G, which is far beyond the threshold value $B_d \approx 300$ G obtained by Aurière et al. (2007), and $B_d \approx 1500$ G obtained

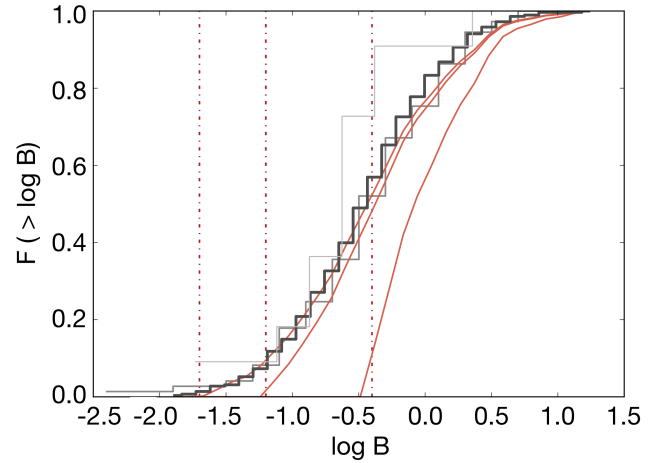


Fig. 8 Cumulative distributions and magnetic thresholds for data from different papers (from left to right: Wade et al. 2015; Aurière et al. 2007; Kholtygin et al. 2010a).

by Kholtygin et al. (2010a). Based on the presented considerations, we also conclude that there is no evidence for any ‘magnetic threshold’ at least for BA and late B-type stars.

On the other hand, Wade et al. (2015) reported preliminary results on a study where a modeling approach by Petit & Wade (2012) has been applied to infer upper limits on dipole magnetic fields in a sample of O-type stars from the MiMeS survey. The results of Wade et al. 2015 imply upper limits on surface dipoles of about 40 G at 50% confidence, and 105 G at 80% confidence. The later values are more consistent with the empirical distributions (Fig. 8). Therefore, we cannot rule out the possibility that the critical value for a magnetic field may exist, but this value should be much lower than proposed earlier.

4.2 Constrains on dissipation of stellar magnetic fields

An important result of our analysis of the empirical magnetic fields distributions is that the time scale of the mag-

netic fields dissipation should be at least comparable with the lifetime of a star on the main sequence. Using the technique of simultaneous fitting we found that the dissipation parameter has to be greater than 0.5 to be consistent with the empirical distributions. This result is in a good agreement with the value obtained by Kholtygin et al. (2010b). However, we cannot estimate the dissipation parameter τ_d more precisely with the current sample of magnetic stars. It means that models with moderate dissipation and without the dissipation all are equally consistent with the empirical data.

We would also like to note, that according to Landstreet et al. (2008), the mean magnetic fields of early A- and late B-type stars decrease by a factor of 3–4 in the range $\tau \in (0.0-0.2)$ and then remain almost constant. The dissipation parameter in that case would be lying within the range of 0.1–0.2 and, according to our simulations, would produce a highly asymmetrical shape of the magnetic field function, inconsistent with the empirical distributions. We believe that this discrepancy may be explained by a limited size of the magnetic stars sample used in their analysis.

4.3 Intrinsic magnetic field function for early-type stars

As we discussed earlier, the empirical distributions are very similar in their appearance. Moreover, it is possible to successfully describe all three of our samples of magnetic stars with a single model. Thus, we consider the possibility that magnetic properties of early type massive stars may be explained by a common magnetic field function *that would be the same* in a very wide range of masses ($\gtrsim 2M_\odot$).

Another strong evidence supporting this hypothesis is that the occurrence of early type magnetic stars is remarkably constant and does not depend on a spectral type or mass of a star. The incidence of magnetic BA stars – which is slightly less than ten per cent – has been known for some time (Wolff 1968; Power et al. 2008).

Recently similar magnetic field detection rates were reported for early B- and O-type stars by the BOB (Schöller et al. 2017) and MiMeS collaborations Wade et al. 2016. It is certainly became more evident now that magnetic stars across the upper main sequence share some common physics related to the phenomena of stellar magnetism (see also Wade et al. 2014, 2015). Given the fact that the incidence of magnetic Herbig Ae/Be stars is also estimated as 7% (Wade et al. 2011), we come to the conclusion that magnetic properties of massive stars are probably determined by physical conditions at early stages of pre-main-sequence evolution, perhaps even during protostar formation.

5 Conclusions

Our investigations of the measured magnetic fields and their evolution for an ensemble of galactic OBA stars show that the distribution of these magnetic field for all mentioned

spectral types can be described by a lognormal law. We develop the population synthesis code to model the magnetic field evolution for OBA stars.

After the analysis of the empirical magnetic field distributions using our model we came to the following conclusions:

- The empirical magnetic field distribution for BA stars can be fitted by the lognormal distribution with the mean $\langle \log B \rangle \approx -0.5$ and the standard deviation $\sigma = 0.5$.
- Our model can be used to reproduce the empirical magnetic field and net magnetic flux distributions for OBA stars supposing that the net magnetic flux distributions at ZAMS is lognormal with parameters $\langle \log \Phi \rangle \approx 26.5$ for model without magnetic field dissipation and for a model with dissipation $\langle \log \Phi \rangle \approx 26.9$.
- The dissipation parameter $\tau_d \gtrsim 0.5$ in an accordance with an estimation by Kholtygin et al. (2010b).
- Our modeling shows that there is no *magnetic desert* in the distribution of the magnetic field of OBA star suggested in the past by some authors (e.g., Lignières et al. 2014).

Acknowledgements. ASM, AFK, SF, GGV and GAC thank the RFBR grant 16-02-00604 A for the support. GGV acknowledges the Russian Foundation for Basic Research (RFBR grant N15-02-05183 A)

References

- Alecian, E., Kochukhov, O., Petit, V. et al. 2014, A&A, 567, A28
 Aurière, M., Wade, G. A., Silvester, J. et al. 2007, A&A, 475, 1053
 Babcock H. W., 1947, ApJ, 105, 105
 Bohlender, D. A., Landstreet, J. D., Thompson, I.B. 1993, A&A, 269, 355
 Braithwaite, J., Nordlund, A. 2006, A&A, 450, 1077
 Bychkov, V. D., Bychkova, L.V., Madej, J. 2009, MNRAS, 394, 1338
 Cash, W. 1979, ApJ, 228, 939
 Castro, N., Fossati, L., Hubrig, S. et al. 2015, A&A, 581, A81
 de la Chevrotière, A., St-Louis, N., Moffat, A. F. J. 2014, ApJ, 781, 73
 Donati, J.-F., Babel, J. Harries, T. J. et al. 2002, MNRAS, 333, 55
 Fabrika, S., Valyavin, G. 1999, 11th European Workshop on White Dwarfs, ASP Conference Series V. 169, Edited by S.-E. Solheim and E. G. Meistas, p. 214
 Ferrario, L., Wickramasinghe, D. 2006, MNRAS, 367, 1323
 Fossati, L., Zwintz, K., Castro, N. et al. 2014, A&A, 562, A143
 Fossati, L., Castro, N., Morel, T. et al. 2015, A&A, 574, A20
 Fossati, L., Castro, N., Schöller, M., Hubrig, S. et al. 2015, A&A, 582, A45
 González, J. F., Hubrig, S., Przybilla, N. et al.: 2017, MNRAS, 467, 437
 Hubrig, S., Schöller, M., Kharchenko, N. V. et al.: 2011, A&A, 528, A151
 Hubrig, S., Schöller, M., Ilyin I., Kharchenko N. V., Oskinova, L. M. et al.: 2013, A&A, 551, A33
 Hubrig, S., Scholz, K., Hamann, W.-R. et al. 2016, MNRAS, 458, 3381
 Hurley, J. R., Pols, O. R., Tout, C. A. 2000, MNRAS, 315, 543
 Igosheva, A. P., Kholtygin, A. F. 2011, AN, 332, 1012

- Kholtygin, A. F., Fabrika, S. N., Drake, N. A. et al. 2010, *AZh*, 36, 370
- Kholtygin, A. F., Fabrika, S. N., Drake, N. A. et al. 2010, *Kin. Phys. Cel. Bod.*, 26, 181
- Kholtygin, A. F. Drake, N. A., Fabrika, S. N. 2010, *Magnetic Stars. Proc. Intern. Conf., held in the Special Astrophysical Observatory of the Russian AS, August 27- September 1, 2010*, Eds: I. I. Romanyuk and D. O. Kudryavtsev, p. 239
- Kholtygin, A. F., Fabrika, S. N., Rusomarov, N. et al. 2011, *AN*, 332, 1008
- Kholtygin, A. F., Fabrika, S., Hubrig, S. et al. 2016, *Stars: From Collapse to Collapse, Proc.Conf. held at Special Astrophysical Observatory, Nizhny Arkhyz, Russia 3-7 October 2016*. Edited by Yu. Yu. Balega, D.O. Kudryavtsev, I. I. Romanyuk, and I. A. Yakunin. San Francisco: Astronomical Society of the Pacific, 2017, p.261
- Kroupa, P. 2002, *Sci*, 295, 82
- Landstreet, J. D., Bagnulo, S., Andretta, V., Fossati, L., Mason, E., Silaj, J., Wade, G. A. 2007, *A&A*, 470, 685
- Landstreet, J. D., Silaj, J., Andretta, V. et al. 2008, *A&A*, 481, 465
- Lignières, F., Petit, P., Auriere, M. et al. 2014, *Magnetic Fields throughout Stellar Evolution, Proc. IAU Symp. V. 302*, 338
- Manchester, R. N., Hobbs, G. B., Teoh, A., Hobbs, M. 2005, *ATNF Pulsar Catalogue*, <http://www.atnf.csiro.au/research/pulsar/psrcat/>
- Monin, D. N., Fabrika, S. N., Valyavin, G. G. 2002, *A&A*, 396, 131
- Morel, T., Castro, N., Fossati, L., Hubrig, S., Langer, N., Przybilla, N., Schöller M. et al. 2014, *Messenger*, 157, 27
- McGill SGR/AXP Online Catalog, <http://www.physics.mcgill.ca/~pulsar/magnetar/main.html>
- Pasineti Fracassini, L E., Pastori, L., Covino, S., Pozzi, A. 2001, *A&A*, 367, 521
- Pelupessy, F. I., van Elteren, A., de Vries, N., McMillan, S. L. W., Drost, N., Portegies Zwart, S. F. 2013, *A&A*, 557, A84
- Pols, O. R., Schröder, K.-P., Hurley, J. R., Tout, C. A., Eggleton, P. P. 1998, *MNRAS*, 298, 525
- Petit, V., Wade, G. A. 2012, *MNRAS*, 420, 773
- Petit, V., Owocki, S.P., Wade, G. A. et al. 2013, *MNRAS*, 429, 398
- Power, J., Wade, G. A., Aurière, M., Silvester, J., Hanes, D. 2008, *CoSka*, 38, 443
- Preston, G. W. 1967, *ApJ*, 150, 547
- Schöller, M., Hubrig, S., Fossati, L. et al. 2017, *A&A*, 599, A66
- Wade, G. A., Alecian, E., Grunhut, J., Catala, C., Bagnulo, S., Folsom, C. P., Landstreet, J. 2011, *ASPC*, 449, 262
- Wade, G. A., Grunhut, J., Alecian, E. et al. 2014, *Magnetic Fields throughout Stellar Evolution, Proc. IAU Symp. V. 302*, pp. 265
- Wade, G. A. et al. 2015, *ASPC*, 494, 30
- Wade, G. A. Neiner, C., Alecian, E. et al. 2016, *MNRAS*, 456, 2
- Wolff, S. 1968, *PASP*, 80, 281